Portugaliae Electrochimica Acta 2019, 37(4), 241-255

DOI: 10.4152/pea.201904241

PORTUGALIAE ELECTROCHIMICA ACTA
ISSN 1647-1571

Electrochemical and Computational Studies for Mild Steel Corrosion Inhibition by Benzaldehydethiosemicarbazone in Acidic Medium

Taghried A. Salman, Khalida A. Samawi and Jawad K. Shneine*

Department of Chemistry, College of Science, Al-Nahrain University, Baghdad, Iraq

Received July 21, 2017; accepted January 2, 2018

Abstract

The inhibiting effect of benzaldehydethiosemicarbazone (BTSC) on the mild steel alloy corrosion in a 1 M sulfuric acidic solution was potentiostatically investigated at four temperatures, in the range of 298.15 to 328.15 K. Three BTSC concentrations, ranging from 100 to 300 mg/L, were tested. Mild steel corrosion feasibility decreases with increasing inhibitor concentrations, and also with the rise in temperature. A protection efficiency of 96% was obtained at 300 mg/L, and 328.15 K. Potentiostatic polarization studies showed that BTSC acted as a mixed type inhibitor. The main kinetic effect of the BTSC inhibitor added to the sulfuric acid solution was to considerably enhance activation energy values, pre-exponential factor and activation entropy of the alloy corrosion. This was because BTSC shifted the corrosion reaction on the mild steel surface to reaction sites where energy was relatively higher than that on which the corrosion occurred in the inhibitor absence. The inhibitor adsorption followed the Langmuir adsorption isotherm. The activation thermodynamic functions (E_a, K_{ads}, $\Delta G_{ads.}$, $\Delta H_{ads.}$ and ΔS_{ads}) were evaluated. The obtained activated parameters revealed that BTSC adsorption took place through chemisorption. Scanning electron microscopy (SEM) technique was used to provide insight into the formation of a protective film on the alloy surface. To provide a relationship between the BTSC's molecular structure and its corrosion inhibition capability, quantum chemical studies were achieved using density functional theory (DFT) at the B3LYP/6-311G level.

Keywords: mild steel; BTSC; potentiostatic polarization; inhibitor; SEM; quantum chemical calculations.

Introduction

Steel corrosion is an essential industrial and academic topic that has gained an extensive attention [1]. Mild steel has been widely used in chemical industries, for many purposes under different environments, in handling alkalis, acids, and salt solutions [2]. Hydrochloric and sulfuric acids are widely used for this purpose. However, most acidic media cause metal corrosion [1]. Mild steel

* Corresponding author. E-mail address: jkshneine@gmail.com

corrosion inhibition in acidic solutions can be considered as one of the most serious solutions to decrease metal corrosion and excess acid consumption [3].
Generally, heterocyclic organic compounds, comprising oxygen, nitrogen, or sulfur hetero atoms and an electron conjugated system, are mostly applied as efficient corrosion inhibitors to retard mild steel alloys retrogradation [4]. The molecules adsorption onto the metallic surface can be considerably determined by the valence shell lone pairs in heteroatoms and by the geometrical planarity [5]. The corrosion inhibition efficiencies strongly depend on the inhibitor capability to adsorb onto the metal surface, and on the chemical, physical and structural properties of organic molecules [6].
Excellent corrosion inhibition can be obtained using organic compounds, which can form coordinate covalent bonds by connecting their occupied valence shell electrons to unoccupied metal surface d-orbitals, and accept free electrons from the metal surface, using unoccupied anti-bonding orbitals and forming resistant bonds [7-8].
In order to elucidate the electronic structure and reactivity, and to determine the molecular structure, it is very useful to apply quantum chemical methods [9]. Density functional theory (DFT) can be considered as a very useful model to explain, predict and understand numerous features of chemical processes [10-12]. Generally, applied chemical reactivity functional elements, such as softness or hardness and electronegativity can be naturally shown in the DFT method [13]. The inhibitor functionality is strongly related to its frontier molecular orbital (FMO), involving lowest unoccupied molecular orbital (LUMO), highest occupied molecular orbital (HOMO), and other factors, such as softness or hardness. Theoretical investigations using quantum chemical methods have successfully explained and determined the relationship between corrosion inhibition efficiency and molecular orbital (MO) energy levels for specific types of organic molecules [14].
In the present work, the inhibiting effect of benzaldehyde thiosemicarbazone (BTSC) (Fig. 1) on mild steel corrosion in a 1 M H_2SO_4 solution, at four different temperatures in the range from 298.15 to 328.15 K, was investigated. Theoretical and electrochemical experiments were herein applied.

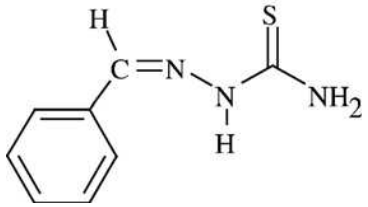

Figure 1. BTSC chemical structure.

The dependence of the corrosion rate on temperature, enabling corrosion activation energies, as well as the activation entropy, was also studied. Thermodynamic quantities of mild steel corrosion in an acidic solution under study were calculated from the appropriate corrosion potential values, and their variation with temperature. The relationships between corrosion inhibition performance and calculated dipole moment (μ), ΔE (E_{HOMO}-E_{LUMO}) gap of

molecular orbitals, charge density on hetero atoms, and bond lengths, as well as some structural parameters, were evaluated.

Experimental section

Materials

A mild steel sheet, with the composition (wt.%) Mn (0.6), P (0.36), C (0.15) and Si (0.03) and the remainder Fe, was used in this work. Coupons with the dimensions of 5×4×0.11 cm were made thereof. Each coupon was degreased by washing it with ethanol, dipped in acetone, dried in the air, and finally kept in a desiccator. A 1 M H_2SO_4 solution was prepared by dilution of concentrated H_2SO_4 with distilled water. Polarization studies were performed in a 1 M H_2SO_4 solution, in the absence and presence of various BTSC inhibitor concentrations, ranging from 100 ppm to 300 ppm. BTSC was purchased from Aldrich, with a purity of 96%.

Polarization measurements

Potentiodynamic polarization experiments were conducted using a complete M Lab 200 potentiostat/galvanostat control station for electrochemical cells. The range settings function generator and operation modes were controlled by an M Lab 200 microcomputer. M Lab 200 is also capable to manage data and to communicate with a connected computer. One serial interface connects to a personal computer; another allows connecting it to other M Labs. The recorded potentiodynamic current-potential curves can be generated by automatic variation of the electrode potential from -800 to -100 mV, at a rate of mVs^{-1}. Firstly, a steady state had to be reached by immersing the working electrode (WE) in the test solution at the natural potential (open circuit potential), for 30 min. In order to remove the oxide film from the electrode, WE was polarized at -800 mV, for 10 min. The corrosion current densities (i_{corr}) were obtained by extrapolation of the linear Tafel segments of the anodic and cathodic curves to the corrosion potential.

The corrosion kinetic parameters were evaluated from the resulting data in the Tafel region by plotting the polarization curves. Thus, the corrosion current values were obtained by extrapolating the linear Tafel segments, in a large potential domain of the cathodic curves to the corresponding corrosion potentials. Correspondingly, the inhibition efficiency was calculated by applying the following relationship:

$$IE_{I\text{-}E} = \frac{i^{\circ}_{corr} - i_{corr}}{i_{corr}} \times 100 \qquad (1)$$

where i°_{corr} and i_{corr} indicate the corrosion current density values without and with inhibitor, respectively. Surface coverage (θ) at a definite inhibitor concentration was obtained from polarization curves, using the following equation [15]:

$$\theta = 1 - i_{corr} / i^{\circ}_{corr} \qquad (2)$$

Scanning electron microscopy (SEM)

The carbon steel surface morphology was evaluated using a FEI Inspect-S50 Scanning Electron Microscopy. Mild steel samples were measured before and after immersion in the sulfuric acid solution, with and without BTSC inhibitor.

Computational tools

In this respect, DFT method has been frequently applied to obtain details for elucidating manifold chemical concepts found in different Chemistry fields. In this work, standard Gaussian 09 software package was applied to achieve quantum chemical calculations on complete geometry optimizations [16]. B3LYP functional at the 6-311G basis set, and at the density functional theory level (DFT), was used to provide geometry optimization. To give a structural designation of the corrosion inhibitor, and to consider the features of the inhibitor/surface mechanism, DFT method was applied [17].

Density functional theory is regarded as a very beneficial method to query the inhibitor/surface interaction, and to examine the experimental results. It can provide the most important qualitative chemical concepts, such as electronegativity (χ) and hardness (η) [11]. The following equation explains the context of the density functional theory of chemical reactivity, which associates the electronic chemical potential (μ) to electronegativity (χ) [18].

$$\mu - \left(\frac{\partial 2E}{\partial N}\right)v(r) - -X \qquad (3)$$

where N = number of electrons, ν(r) = external potential and E = total energy.

DFT defined hardness (η) as the second derivative of E regarding N at V(r) property, which measures both the molecule's reactivity and stability [19].

$$\eta = \{\partial^2 E/\partial N^2\}\, V(r) \qquad (4)$$

The electron affinity (EA) and ionization potential (IE) of the inhibitor molecules were determined according to Koopman's theorem, using the following equivalences, for χ and η being evaluated [20]:

Ionization energy (IE) = - Energy of the highest occupied molecular orbital ($-E_{HOMO}$)
Electron affinity (EA) = - Energy of the lowest unoccupied molecular orbital ($-E_{LUMO}$)

In the reactions with electrophiles, E_{HOMO} can be considered as the more reactive molecule, whereas E_{LUMO} is indispensable for molecular reactions with nucleophiles [21].

$$\text{Electronegativity } (\chi) = \text{IE+EA}/2 \qquad (5)$$
$$\text{Hardness } (\eta) = \text{IE-EA}/2 \qquad (6)$$

The global softness (S) is defined as the inverse of the global hardness [22]:

$$\text{Global softness (S)} = 1/\eta \qquad (7)$$

$$\Delta N = \frac{\chi Fe - \chi inh}{[\eta Fe + \eta inh]} \qquad (8)$$

In the chemical reactivity concept, electronegativity, hardness and softness are very convenient quantities. By joining together the inhibitor molecule and the metallic atom, electrons are capable to stream from χ (inhibitor) lower value to χ (Fe) higher value, until their chemical potentials have the same value. According to Pearson, the electron fraction (ΔN) transfer from the inhibitor molecule (BTSE) to the metal was calculated [23]. ΔN was calculated using the above mentioned formula [24].

Where η_{inh} and η_{Fe} are the absolute hardness of the inhibitor molecule, and iron, and χ_{inh} and χ_{Fe} are the absolute electronegativity of the inhibitor molecule, and iron, respectively. In this work, the theoretical values of χ_{Fe} = 7.0 eV and η_{Fe} = 0 were used for calculating the number of transferred electrons [22]. It is assumed that the electron transfer might be driven by the electronegativity differences, while the sum of the hardness parameters can be seen as resistance [25]. Condensed Fukui function can reasonably analyze the local selectivity of a corrosion inhibitor.

Quantum chemical parameters

B3LYP hybrid functional has been often used to estimate a wide range of molecular properties. In this work, parameters and thermochemical properties (atomization energies and reaction energies) have been accurately fixed to calculate B3LYP functional. Gaussian 09 program was used to achieve quantum calculations. The compound geometry to be studied was implemented using the DFT level of the three-parameter compound functional of Becke (B3LYP).The basis 6-311G set for all atoms has been used. The molecule structural geometry was optimized under no constraints. HOMO and LUMO levels were taken out. On the basis of the molecular orbital energies (MO), the difference between HOMO and LUMO levels (the energy gap) was then estimated [26-28].

Results and discussion

Potentiostatic polarization studies

The polarization curves for mild steel corrosion in a 1 M H_2SO_4 solution, at four different temperatures in the range of 298-328 K, are indicated in Fig. 2. The data derived from the polarization curves are corrosion potentials (E_{corr}), currents (i_{corr}), cathodic (b_c) and anodic (b_a) Tafel regions. Table 1 shows the data derived from the polarization curves for mild steel in a 1 M H_2SO_4 solution, at different temperatures under study. Based on Table 1, E_{corr} values moved to more negative potentials with increasing temperatures. The shift in the corrosion potential towards the active (more negative) direction generally implies a reduction in corrosion resistance. Furthermore, the corrosion current density (i_{corr}) increases with higher temperatures, indicating an increasing reaction rate with the rise in temperature.

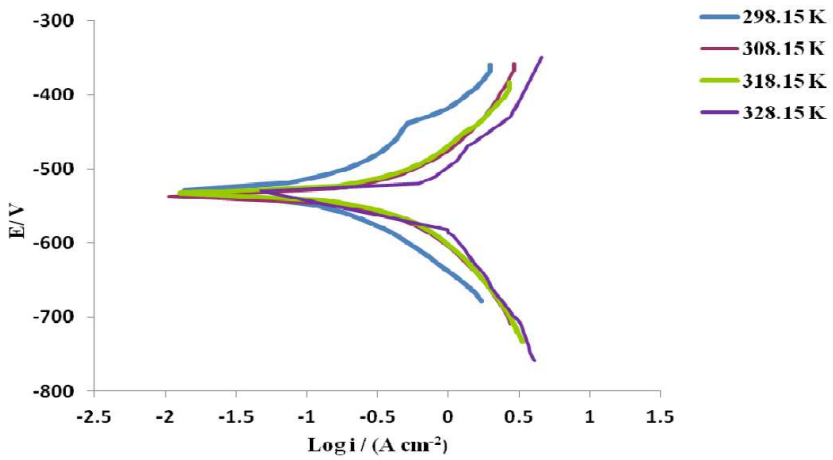

Figure 2. Typical polarization curve for mild steel corrosion in a 1 M H_2SO_4 solution, at four temperatures in the range from 298 to 328 K.

Table 1. Data obtained from the potentiostatic polarization curves for mild steel corrosion in a 1 M H_2SO_4 solution, in the absence and presence of different BTSC concentrations, at four different temperatures in the range from 298 to 328 K.

Conc./ppm	T/K	(i_{corr})/ 10^{-4} A.cm^{-2}	-E_{corr} (V vs. SCE)	-b_c/ V. decade^{-1}	b_a/ V. decade^{-1}	θ	P%
None	298.15	1.12	0.530	0.103	0.085	-	-
	308.15	1.73	0.561	0.110	0.090	-	-
	318.15	2.91	0.585	0.115	0.095	-	-
	328.15	3.62	0.612	0.132	0.102	-	-
100	298.15	0.140	0.384	0.179	0.108	0.875	87.50
	308.15	0.160	0.399	0.182	0.127	0.907	90.75
	318.15	0.230	0.464	0.193	0.153	0.921	92.09
	328.15	0.320	0.485	0.202	0.174	0.922	92.23
200	298.15	0.1232	0.392	0.185	0.110	0.890	89.00
	308.15	0.1380	0.425	0.191	0.144	0.920	92.00
	318.15	0.2037	0.471	0.204	0.171	0.930	93.00
	328.15	0.2624	0.497	0.217	0.196	0.936	93.63
300	298.15	0.1008	0.411	0.194	0.132	0.910	91.00
	308.15	0.1038	0.432	0.206	0.165	0.940	94.00
	318.15	0.1164	0.490	0.215	0.184	0.960	96.00
	328.15	0.1350	0.508	0.228	0.201	0.967	96.72

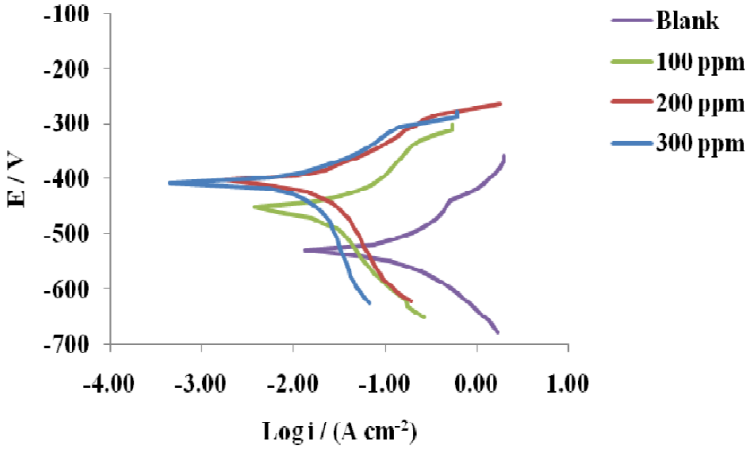

Figure 3. Typical polarization curve for mild steel corrosion in a 1 M H_2SO_4 solution, in the absence and presence of different BTSC concentrations, at 298 K.

Fig. 3 represents typical polarization curves for mild steel in a 1 M H_2SO_4 solution, without and with different BTSC concentrations, at 298 K. The data obtained from polarization curves at various BTSC concentrations, and four temperatures, are shown in Table 1 and Fig. 3. Results obviously show that BTSC addition to a 1 M sulfuric acid solution enhanced the mild steel specimen resistance. Such tendency increases with increasing concentrations of the inhibitor under investigation. On the other hand, increasing temperatures lead to a decrease in the tendency of mild steel for corrosion.
Table 1 shows that both b_a and b_c values increased with increasing temperatures, in the presence of various BTSC concentrations in the sulfuric acid solution. Therefore, interference between anodic and cathodic reactions has occurred in BTSC presence, indicating that the inhibitor acts as a mixed type inhibitor. A cathodic Tafel slope of -0.120 V might diagnose a discharge-chemical desorption mechanism for hydrogen evolution reaction at the cathode, in which the proton discharge should be the rate-determining step. The anodic Tafel slopes (b_a) variation might be ascribed to the variation of the rate-determining step in the metal dissolution reaction. A mechanism and rate-determining step change cannot be ignored throughout the anodic processes.

Protection efficiency

The protection efficiency percentage (P%) of mild steel in 1 M sulfuric acid in the presence of different BTSC concentrations was obtained using equation (1). Table 1 shows the results obtained for various inhibitor concentrations and temperatures. From the results, it appears that the obtained protection efficiencies are increased with increasing inhibitor concentrations and temperatures. This is attributed to the increase in the inhibitor adsorption onto the metal surface, due to increasing temperatures. This behavior reveals chemical adsorption [29].

Corrosion kinetics

Mild steel corrosion rate (r), in the inhibitor absence and presence, might be described by Arrhenius equation.

$$r = A \exp(-E_a / RT) \qquad (9)$$

where A and E_a are the pre-exponential factor and the activation energy, respectively. The value of (r) at any temperature (T) was taken to be conformable to the corrosion current density (i_{corr}). Fig. 4 shows Arrhenius plots for the blank (inhibitor absence) and various inhibitor concentrations; E_a and A values have been derived from the plots slopes and intercepts, respectively. Activation entropy (ΔS^*) was then calculated from A value, using the relationship:

$$A = (kT/h)\, e^{\Delta S^*/R} \qquad (10)$$

where k, h, and R are constants and T is the solution temperature.

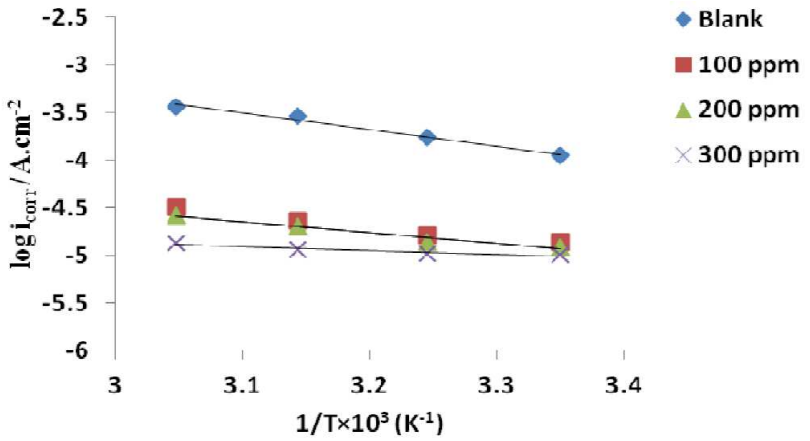

Figure 4. Arrhenius plot relating log i_{corr} with 1/T for mild steel corrosion in a 1 M H_2SO_4 solution, in the absence and presence of various BTSC concentrations.

Table 2 gives E_a, A and ΔS^* resulting values for mild steel corrosion in a 1 M H_2SO_4 solution, in the BTSC inhibitor absence and presence, at different concentrations, and over the temperature range from 298 to 328 K.

Table 2. Activation energy (E_a), pre-exponential factor (A) and activation entropy (ΔS^*) for mild steel corrosion in a 1 M H_2SO_4 solution, in the absence and presence of different BTSC concentrations, over the temperature range from 298 to 328 K.

T / K	**E_a**/kJ.mol^{-1}	**A**/molecules.cm^{-2}.s^{-1}	**ΔS^***/kJ. K^{-1}.mol^{-1}
None			
298.15	36.43	1.65x10^{21}	70.021
308.15			69.912
318.15			69.788
328.15			69.679
100 ppm			
298.15	19.93	2.59x10^{17}	46.730
308.15			38.278
318.15			38.161
328.15			38.053
200 ppm			
298.15	25.95	2.31x10^{18}	54.615
308.15			46.184
318.15			46.068
328.15			45.959
300 ppm			
298.15	27.19	3.16x10^{18}	55.743
308.15			47.307
318.15			47.190
328.15			47.082

The data show that BTSC adsorption onto mild steel, particularly at low concentrations (100 ppm) in the H_2SO_4 solution, was associated to activation energies, which were relatively lower than those obtained in the inhibitor absence. Thus, BTSC presence in the acid at such concentrations probably modifies the corrosion reaction to surface sites where E_a is lower than the normal mild steel activation energy in the inhibitor absence. This may be due to an

electric field arising at the inhibitor/metal interface [30-31], which may lower the energy barrier for the metal corrosion, at such inhibitor concentrations.

Corrosion thermodynamic quantities

The following equation describes the dependence of Gibbs free energy (ΔG) on the metal corrosion potential (E_{corr}), in a definite medium, and at a given temperature [32].

$$\Delta G = - n F E \qquad (11)$$

where F is the Faraday constant, E is the cell potential ($E=E_{corr}$), and n is the number of electrons involved in the corrosion reaction. From ΔG values at different temperatures, for each inhibitor concentrations, it has been possible to estimate ΔS values using the following thermodynamic relation:

$$\Delta S = -d (\Delta G) / dT \qquad (12)$$

The free energy change (ΔG) is related to enthalpy and entropy (ΔH, ΔS) for the corrosion process at a constant temperature, (T), by the equation:

$$\Delta G = \Delta H - T\Delta S \qquad (13)$$

where ΔS represents the plot slope of ΔG values against temperatures, (Fig. 5). The corresponding change values in the enthalpy (ΔH) of the corrosion reaction at each temperature can be calculated using ΔG and ΔS values. Table 3 shows the obtained data.

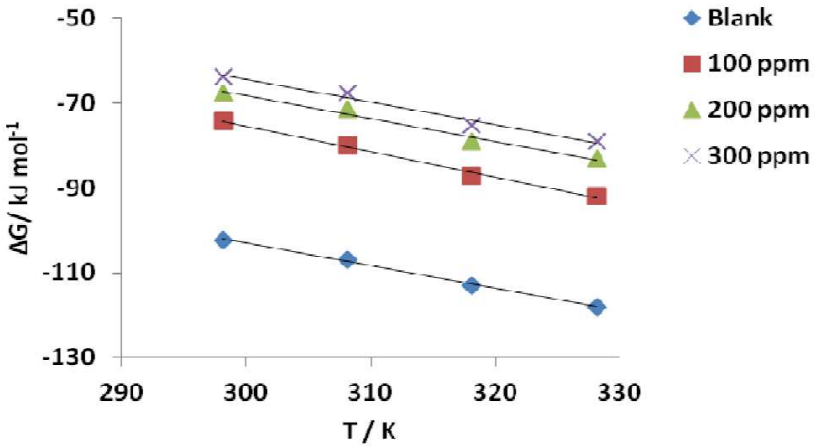

Figure 5. Gibbs free energies (ΔG) variation with temperature for mild steel corrosion in 1 M H_2SO_4 at the absence and presence of different BTSC inhibitor concentrations.

The results presented in Table 3 indicate ΔG negative values, which means that these reactions are spontaneously occurring. The enthalpy changes (ΔH) of the mild steel corrosion reaction in different BTSC concentrations, at temperatures ranging from 298 to 323 K, have negative values, which designate an exothermic reaction. The solvent molecules orientation around the hydrated metal ions in the corrosion medium, and their order, can be described by ΔS values. Due to ΔG

negativity, ΔS values were generally positive. Compared to the metal atoms state in the crystal lattice of the corroding electrodes, this indicates a lower order of the metal ions solvated states [33].

Table 3. Thermodynamic calculations (ΔG, ΔH, ΔS) for mild steel in a 1 M H_2SO_4 solution, in BTSC presence at different concentrations, with four temperatures.

Conc./ppm	T/K	-ΔG (KJ.mol^{-1})	ΔH (KJ.mol^{-1})	ΔS (J.K^{-1}.mol^{-1})
0	298.15	102.29	64.59	560
	308.15	106.83	65.73	
	318.15	112.96	65.20	
	328.15	118.12	65.64	
100	298.15	74.11	107.163	608
	308.15	80.06	107.295	
	318.15	87.13	106.305	
	328.15	92.04	107.475	
200	298.15	67.550	94.644	544
	308.15	71.410	96.495	
	318.15	79.130	94.229	
	328.15	83.140	95.669	
300	298.15	63.690	96.357	536
	308.15	67.550	79.565	
	318.15	75.270	95.513	
	328.15	79.01	97.141	

Surface coverage and adsorption behavior

Mild steel surface coverage (θ) degree in a 1 M H_2SO_4 solution containing different BTSC concentrations, over the temperature range from 298 to 328 K, obtained from equation (2), is shown in Table 1. The obtained data show that the surface coverage linearly varied with the inhibitor concentration, which is suitable to Langmuir adsorption isotherm [34] that can ideally describe physical or chemical adsorption. According to the following equation, Langmuir assumption is related to the electrolyte (C) adsorbate concentration ratio to the surface coverage degree (θ):

$$C/\theta = 1 / K_{ads} + C \qquad (14)$$

where K_{ads} is the equilibrium adsorption constant.

Fig. 6 shows BTSC Langmuir adsorption isotherm in a 1 M H_2SO_4 solution. The linearity in the results at various concentrations with the unity (1) correction factor evidences that BTSC inhibition effect was due to its molecules adsorption onto the mild steel surface. In addition, the inhibitor adsorption behavior is assumed to obey Langmuir adsorption isotherm.

Free adsorption energy (ΔG_{ads}) was calculated at the temperature range from 298 to 328 K, using the relation:

$$K_{ads.} = \frac{1}{55.55} \; e^{(-\Delta G_{ads} / RT)} \qquad (15)$$

K_{ads} and ΔG_{ads} calculated values are presented in Table 4.

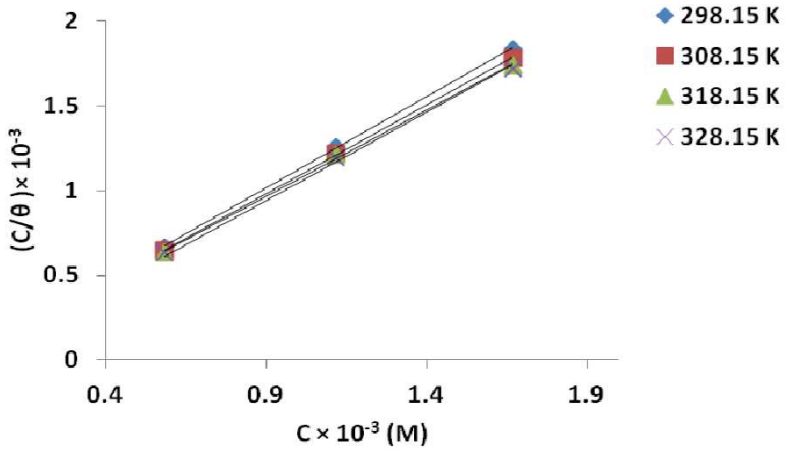

Figure 6. Langmuir isotherm plot of BTSC adsorption onto mild steel surface in a 1 M H_2SO_4 solution, at various temperatures in the range of 298-328 K.

Table 4. Thermodynamic parameters for BTSC inhibitor adsorption onto the mild steel surface in a 1 M H_2SO_4 solution.

T/K	k_{ads}/(M^{-1})	$-\Delta G_{ads}$/(kJ.mol^{-1})	$-\Delta H_{ads}$/(kJ.mol^{-1})	ΔS_{ads}/(J.K^{-1}.mol^{-1})
298.15	3448.28	30.15	3.84	114
308.15	3703.70	31.34	3.79	
318.15	3846.15	32.46	3.81	
328.15	4000.00	33.59	3.82	

The negative values of free adsorption energy indicate a spontaneous adsorption process; ΔG_{ads} values are around -30 k J mol^{-1}, confirming that BTSC adsorption onto the mild steel surface is physisorption. Thermodynamic parameters were obtained from Gibbs-Helmholtz equation, as follows:

$$\Delta G_{ads.} = \Delta H_{ads.} + T\,\Delta S_{ads.} \qquad (16)$$

Plots of ΔG_{ads} vs. T for BTSC adsorption onto the mild steel surface in a 1 M H_2SO_4 solution, over the temperature range from 298 K to 328 K, are shown in Fig. 7 and in Table 4. The data gave a straight slope line (ΔS_{ads}) and, in every temperature, ΔH_{ads} can be calculated.

ΔH_{ads} negative values indicate that the adsorption process is exothermic. Generally, an exothermic adsorption process signifies either physisorption or chemisorptions, while the endothermic process is attributed to chemisorption. In addition, the inhibitor molecules adsorption is accompanied by ΔS_{ads} positive values.

SEM evaluation

Scanning electron microscopy was used to investigate the carbon steel specimen surface morphology. Fig. 8 shows a SEM representation for the polished carbon steel surface, before and after the corrosion experiment in the inhibitor absence, and in the presence of 300 ppm of inhibitor in a 1 M H_2SO_4 solution, at 298.15 K (Fig.8 (a, b, c), respectively). From Fig. 8a, the polished carbon steel electrode surface was uniform. After immersion in 1 M H_2SO_4, the surface was strongly

damaged, due to the corrosion (Fig. 8b). In BTSC presence, thin films onto the carbon steel surface were formed, as shown in Fig. 8c. It is indicated that there is a protective layer adsorbed onto the carbon steel surface, which is responsible for corrosion inhibition.

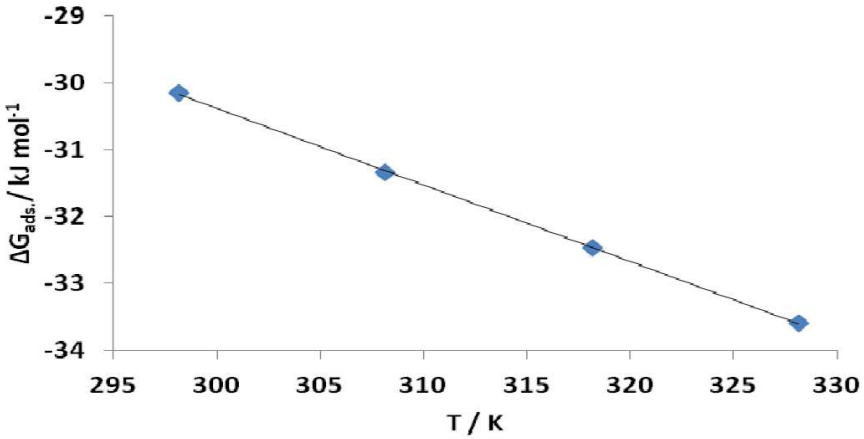

Figure 7. Gibbs free energies ($\Delta G_{ads.}$) variation with temperature for BTSC adsorption onto mild steel surface in a 1 M H_2SO_4 solution.

Table 5. Calculated quantum chemical parameters of the studied BTSC inhibitor with mild steel in 1 M H_2SO_4, using DFT method.

Highest occupied molecular orbital (E_{HOMO})/eV	-5.346
Lowest unoccupied molecular orbital (E_{LUMO})/eV	-1.831
$\Delta E(E_{LUMO} - E_{HOMO})$ /eV	3.515
Dipole moment (μ)/ Debye	5.923
Ionization energy (IE) /eV	5.346
Electron affinity (EA) /eV	1.831
Electronegativity for inhibitor(χ)	3.589
Hardness for inhibitor (η)	1.766
Electron transfer (ΔN)	0.965
Total energy(E_{total}) kcal/mol	-5474.78

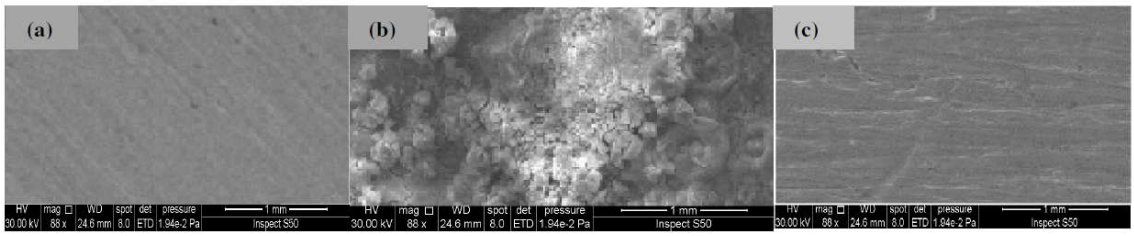

Figure 8. SEM micrographs, **(a)** of polished mild steel, **(b)** after immersion for 24 h in a 1 M H_2SO_4 solution alone, and **(c)** in the presence of 300 ppm of BTSC inhibitor, at 328.15 K.

Theoretical calculation

The theoretical computational studies were applied to obtain an idea of the theoretical system, reflecting a correlation between the corrosion inhibition functioning and the electronic structure. In this work, the electronic structure model of the inhibitor molecule can be obtained using density functional theory (DFT) computations. The inhibitor structure has been related to theoretical quantum chemical parameters such as E_{HOMO}, E_{LUMO}, and the energy gap

between them ($\Delta E = E_{LUMO} - E_{HOMO}$) [35]. High HOMO values are associated with the capacity of the inhibitor molecule to donate an electron to an acceptor with an empty molecular orbital, which easily renders the adsorption process and, therefore, demonstrates a better reaction of the corrosion inhibitor. E_{LUMO} values are in agreement with the electron acceptance tendency, usually from the metal surface atoms.Therefore, the calculated difference (ΔE = 3.515 eV) shows BTSC molecule ability to donate electrons, which measures the relationship between the metal surface and the inhibitor. BTSC electronic structure and molecular orbitals (MO) have been modeled to prove the active sites as well as the molecule's topical reactivity. The inhibitor optimized structure (HOMO and LUMO orbitals) is shown in Fig. 9 and Table 5. HOMO and LUMO energies for the inhibitor molecule were -5.346 eV and -1.831 eV, respectively. The inhibitor molecule with a high E_{HOMO} value is capable to strongly adsorb onto the metal surface. The high ΔE value (3.515 eV) suggests, in turn, high adsorption ability onto the mild steel.

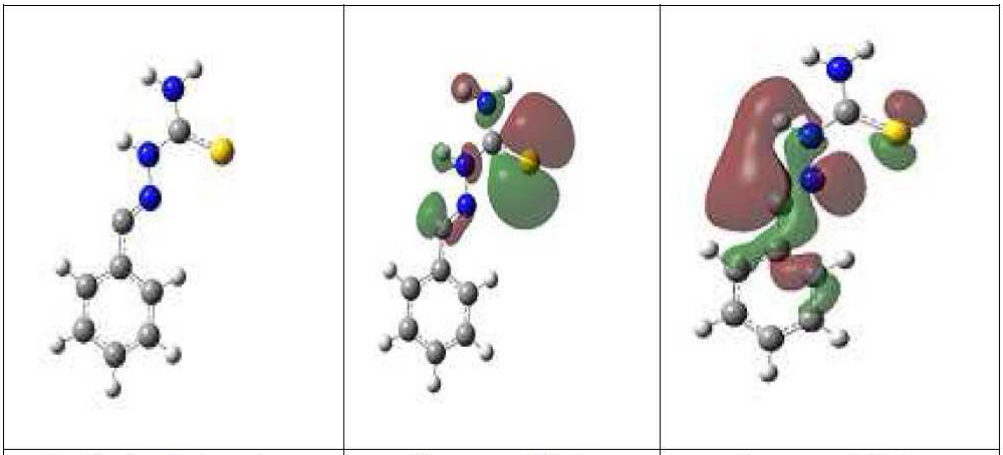

Figure 9. Electronic distribution of BTSC inhibitor (C = grey; H = white; N = blue; and S = yellow).

The inhibitor molecule with the considerably higher dipole moment (μ) value of 5.923 Debye, in comparison with that of H_2O (1.85 Debye), also increases its adsorption ability onto the metal surface [36]. For this reason, it is assumed that a quasi-substitution process occurred between the inhibitor molecule in the aqueous phase, and water molecules at the electrode surface [H_2O (ads)]. The total energy (E_{total}) value of the inhibitor molecule is equal to -5474.7844 Kcal/mol, which indicates a favorably adsorption process through the active sites. Using IE and EA values obtained from quantum chemical calculations, η values were calculated. The fraction of electrons transferred (ΔN=0.9659) from the inhibitor molecule to the iron molecule was calculated. In comparison to previous results, a good inhibition effect resulted from electrons donation, as indicated from ΔN value. The inhibitor molecule is considered as an electron donator, while the steel surface is considered as an acceptor [37-38].

Conclusion

Potentiometric measurements obviously show that BTSC addition, as a corrosion inhibitor to a 1 M sulfuric acid solution, enhanced the mild steel specimen resistance. A cathodic Tafel slope of -0.120 V might diagnose a discharge-chemical desorption mechanism for hydrogen evolution reaction at the cathode, in which the proton discharge should be the rate-determining step. Obtained protection efficiencies were increased with higher inhibitor concentrations and temperatures. ΔH_{ads} negative values indicate an exothermic adsorption process and, therefore, reveal chemical adsorption. SEM measurements firmly indicate a protective layer adsorbed onto the carbon steel surface, which is responsible for the corrosion inhibition. A strong inhibitor adsorption onto the metal surface is also confirmed by quantum chemical calculations. Molecule planarity and heteroatoms presence seem to be the potential elements that designate the strong molecular adsorption capability and inhibitory power.

Acknowledgments

The Department of Chemistry, College of Science of Al-Nahrain University, is gratefully acknowledged for the financial support and for providing required materials and apparatus needed to achieve this work.

References

1. Abd El-Maksoud SA, Fouda AS. Mater Chem Phys. 2005; 93: 84-90.
2. Praveen BM, Venkatesha TV. Int J Electrochem Sci. 2009; 4: 267-275.
3. Jayaperuma D. Mater Chem Phys. 2010; 119: 478-484.
4. Obot IB, Obi-Egbedi NO. Surf Rev Lett. 2008; 15: 903-910.
5. Abd El-Rehim SS, Ibrahim MAM, Khaled FFJ. Appl Electrochem. 1999; 29: 593-599.
6. Wang H, Liu R, Xin I. J Corros Sci. 2004; 46: 2455-2466.
7. Ebenso EE, Isabirye DA, Eddy NO. Int J Mol Sci. 2010; 11: 2473-2498.
8. Valdez LMR, Villafane AM, Maitnik DG. J Mol Struct. 2005; 716: 61-65.
9. Kraka E, Cremer D. J Am Chem Soc. 2000; 122: 8245-8264.
10. Hohenberg P, Kohn W. Phys Rev B. 1964; 136: 864-871.
11. Parr RG, Yang W. Density Functional Theory of Atoms and Molecules. New York: Oxford University Press; 1989.
12. Perdew JP, Ruzsinszky A, Tao J, et al. J Chem Phys. 2005; 123: 62201-62209.
13. Sanderson RT. J Am Chem Soc. 1952; 74: 272-274.
14. Arslan T, Kandemirli F, Ebenso EE, et al. Corros Sci. 2009; 51: 35-47.
15. Mayakrishnan G, Pitchai S, Raman K, et al. Ionics. 2011; 17: 843−852.
16. Benabdellah M, Hammouti B, Warthan A, et al. Int J Electrochem Sci. 2012; 7: 3489-3500.
17. Aouine Y, Sfaira M, Touhami ME, et al. Int J Electrochem Sci. 2012; 7: 5400-5419.

18. Fuchs-Godec R, Pavlovic MG, Tomic MV. Ind Eng Chem Res. 2012; 51: 274-284.
19. Akalezi CO, Enenebaku CK, Oguzie EE. J Mater Environ Sci. 2013; 4: 217-226.
20. Andreev YY. Prot Met Phys Chem Surf.2012; 48: 42-51.
21. Cao JD, Laws KJ, Birbilis N, et al. Corros Engin Sci Technol. 2012; 47: 329-334.
22. Laarej K, Bouachrine M, Radi S, et al. E-J Chem. 2010; 7: 419-424.
23. Barouni K, Bazzi L, Salghi R, et al. Mater Lett. 2008; 62: 3325-3327.
24. Chetouani A, Aouniti A, Hammouti B, et al. Corros Sci. 2003; 45: 1675-1684.
25. Hassani S, Roberts KP, Shirazi SA, et al. Corrosion. 2013; 68: 885-896.
26. Bouklah M, Harek H, Touzani R, et al. Arab J Chem. 2012; 5: 163-166.
27. Boussalah N, Ghalem S, El Kadiri S, et al. Res Chem Interm. 2012; 38: 2009-2023.
28. Chen SK, Scheiner S, Kar T, et al. Int J Electrochem Sci. 2012; 7: 7128-7139.
29. Abdallah M, Helal EA, Fouda AS. Corros Sci. 2006; 48: 1639-1654.
30. Finšgar M, Jackson J. Corros Sci. 2014; 86: 17-41.
31. Cabrera N, Mott NF. Rep Progr Phys. 1948; 12: 163-184.
32. Aslam M, Rais S, Alam M, et al. J Chem. 2013; 2013: 1-11.
33. Shrier LL, Jarman RA. Corrosion Metal/Environment Reactions. Vol 1. 3rd ed. Oxford, Boston: Butterworth-Heinemann; 1994.
34. Bobina M, Kellenberger A, Millet J-P, et al. Corrosion resistance of carbon steel in weak acid solutions in the presence of L-histidine as corrosion inhibitor. Corrosion Science. 2013; 69: 389-395.
35. Oguzie EE, Wang SG, Li Y, et al. Influence of iron microstructure on corrosion inhibitor performance in acidic media. J Phys Chem C. 2009; 113: 8420-8429.
36. Ramji K, Cairns DR, Rajeswari S. Synergistic inhibition effect of 2-mercaptobenzothiazole and Tween-80 on the corrosion of brass in NaCl solution. Appl Surf Sci. 2008; 254: 4483-4493.
37. Ju H, Kai Z, Li Y. Aminic nitrogen-bearing polydentate Schiff base compounds as corrosion inhibitors for iron in acidic media: A quantum chemical calculation. Corros Sci. 2008; 50: 865-871.
38. Lukovits I, Kalman E, Zucchi F. Corrosion Inhibitors-Correlation between Electronic Structure and Efficiency. Corrosion. 2001; 57: 3-8.